Carpio-Cobo, P.; Pawlowski, L.; Pateyron, B. (2019). Numerical investigation of influence of precursors on transport properties of the jets used in solution precursor plasma spraying. Surface and Coatings Technology. 371:131-135. https://doi.org/10.1016/j.surfcoat.2018.09.073

Numerical investigation of influence of precursors on transport properties of the jets used in solution precursor plasma spraying

Pablo Carpio[1,2*], Lech Pawłowski[2] and Bernard Pateyron[2]

1 - Instituto de Tecnología de Materiales (ITM), Universitat Politèctica de Valèencia, Valencia. Cami de Vera s/n 46022, Valencia, Spain

2 - Science des Procédés Céramiques et Traitement de Surfaces (SPCTS), UMR CNRS 7315, Université de Limoges. 12 rue Atlantis 87068, Limoges, France

[*] **Corresponding author**: Pablo Carpio

Address: Instituto de Tecnología de Materiales (ITM). Ciutat Politècnica de la Innovació, ed 8B semisótano, Cami de Vera s/n, 46022, Valencia, Spain.

Tel. number: (+34) 660806113 Fax number: (+34) 963877629

Email address: pabcarco@upv.es

ABSTRACT

The solution precursor plasma spraying is a modification of the conventional plasma spraying technique where the feedstock is a liquid precursor instead of a powder. The phenomena which occur in both techniques are different since the feedstock is liquid and consequently, the jet fragmentation, the solvent evaporation and the chemical reaction or pyrolysis must occur before solid melting and impact onto the substrate. The evaporation of the precursor changes the chemical composition of the plasma plume, hence it implies an important modification in the thermodynamic properties. In the present study, the influence of the solution precursor on these properties, concretely the thermal conductivity and dynamic viscosity of the plasma plume, has been addressed. Then, the ability of heating factor of the plasma plume was estimated and different effects of the precursor on the mentioned transport properties were evaluated.

The effect of the type of precursor, the feedstock flow rate and the solution concentration has been evaluated in the present work. It is concluded that all of these variables affect slightly the viscosity but considerably the thermal conductivity and the ability of heating factor. Hence, the selection of the precursor characteristics allows to heat transfer between plasma plume and starting feedstock and consequently the resultant coatings exhibit a lower presence of porous or unmelted material.

KEYWORDS: Transport properties; solution precursors; plasma spraying

1. Introduction

The solution precursor plasma spraying (SPPS) is an emerging technique enabling manufacturing of nanostructured coatings. It is a modification of the conventional atmospheric plasma spraying (APS) where the feedstock is injected inside a plasma plume and the material is melted and accelerated up to the impacting onto the substrate. Studies have been performed employing SPPS for producing materials intended for desired application such as thermal barrier coatings [1,2], gas sensors [3,4], biomaterials [5,6], etc. SPPS coatings display improved properties with respect to their APS counterparts because of the fine microstructure characteristic in this kind of coatings. The differences between APS and SPPS technique is based on the feedstock a solution precursor instead of a powder; therefore, the process changes considerably. On one hand, the liquid nature of the feedstock implies the injection process is changed and a liquid jet is injected which must be fragmented and the solvent must be evaporated before solid melting. On the other hand, the feedstock consistsof a precursor, ~~which~~ whose composition is transformed inside the plasma plume. It means a chemical reaction or pyrolysis occurs and depending on the kinetics and the hea-transfer, the phenomenon changes and it affect he final coating [7–9].

The microstructure and properties of the coating depends on the starting feedstock as well as the deposition process [10–12]. One of the keys in the process is the heat transfer between the material and the plasma plume, it means that both material and plasma plume properties are affected in this step. Concretely, the plasma plume characteristics which are related with the heat and momentum transfer, called transport properties, are the thermal conductivity and the dynamic viscosity [13–15]. They depends basically on the chemical composition of the plasma plume but the environment also affects. For example, vapors generated during the process vary the

chemical composition of the plume; therefore, the transport properties are modified. This is the case of the SPPS process where the solvent and the sub-products of the precursor decomposition become part of the plume.

In spite of fact the that the SPPS technique is being studied since 2001, more studies to know the technique are necessary. Several works have dealt with the development and evaluation of SPPS coatings but the examination of the thermo-physical changes inside the plasma plume has been limited. Experimental examination of these phenomena is difficult because of the high temperature of the plasma jet and rapidity of the reaction. In this way, some numerical modeling works on the transformation of droplets in SPPS have been reported [16,17]. However, the analysis of thermodynamic properties must also be considered. Previous researches have addressed the change in the transport properties experimented in the plasma plume when the feedstock is a suspension instead of a powder in the case of suspension plasma spraying [18,19]. Hence, the aim of the present study is the evaluation of the transport properties injecting a solution precursor. Besides, the influence of the type of precursor and its concentration, as well as the effect of the feedstock flow rate, is also analyzed. This study was focused on precursors commonly used to develop zirconia coatings since this material is important owing to its applications as thermal barrier or solid oxide fuel cell's electrolyte [1,2,20]. Nevertheless, the obtained conclusions can be translated to any kind of coating developed by SPPS.

2. Methodology

2.1. Feedstock and spray parameters

The feedstocks considered in the present work consisted of ZrO_2 precursors. Concretely, three of the most used precursors (one organic and two inorganic ones) were selected

for the evaluation. Moreover, the effect of the solution molarity as well as the feedstock flow rate was examined. Water was taken as diluting agent although ethanol or other agents can be considered. It is important because it affects considerably the thermal transport properties, as it was demonstrated in a previous the work [19]. Table 1 displays the kind of precursors as well as the molarity and flow rate values contemplated in the thermal transport estimations. The range of these values and the precursors were taken from previous experimental works about SPPS coatings [2,5,21,22].

The plasma spray parameters remained constant because their optimization was not the objective of this study. Argon and hydrogen were selected as primary and secondary plasmogen gases and their flow rates were 45 and 5 slpm respectively. A monocathode nozzle with a diameter of 9 mm was considered and the electrical power was 40 kW. All of these parameters, like feedstock conditions, were taken from our previous works [5]. The molar fraction of precursors and working gas were calculated in order to estimate the plasma plume properties.

2.2. Estimation of transport properties

The transport properties described the fluxes such as mass, electric charges and thermal energy which enable to predict the gas system. The transport properties related to momentum and heat transfer are the dynamic viscosity and the thermal conductivity respectively. Dynamic viscosity (η_g), [Pa·s] or [kg/(m·s)], is a coefficient of

proportionality between the friction force (F) and its consequent gradient of gas velocity ($\frac{\delta v_{g,x}}{\delta x}$):

$$F = \eta_g \left(\frac{\delta v_{g,x}}{\delta x}\right) \quad (1)$$

Likewise, thermal conductivity (λ_g), [$W \cdot m^{-1} \cdot K^{-1}$], is the coefficient of proportionality between the heat flux (q_x) and the gradient in temperature ($\frac{\delta T_g}{\delta x}$):

$$q_x = \lambda_g \left(\frac{\delta T_g}{\delta x}\right) \quad (2)$$

The transport properties can be guessed from the Boltzmann equation in the Chapman-Enskog approach described elsewhere [23]. The plasma plume characteristics are strongly related to the chemical composition. The different chemical species, both neutral (as Ar, H_2…) and ionic (as Ar^+, H^+, e^-…), inside the plasma plume depends on temperature which results from the balance between the electrical energy dissipated and the heat losses that occur in the plasma plume.

The guesses of chemical composition and transport properties at different temperatures were carried out with the use of T&TWinner software which is feed by a huge database of chemical species. This software established the equilibrium onto minimization of Gibbs's free energy ~~of Gibbs~~ and Chapman-Enskog approach [24].

2.3. Ability of heating factor

The heat transfer from plasma plume to a particle is governed by the convention heating of the plasma around the particle and the conduction heating inside the particle,

supposing that the radiation heating by the plasma and radiation cooling of particles can be neglected [26]. In this case, the heat transfer equation has a form:

$$\pi {d_p}^2 h\left(T_g - T_p\right) = \frac{1}{6}\pi C_p {d_p}^3 \frac{\mathrm{d}T_p}{\mathrm{d}t} \quad (3)$$

where d_p - particle diameter [m], h - heat transport coefficient [W.m^{-2}K^{-1}], T_g and T_p - temperature of plasma and particle respectively [K], C_p - specific heat of particle, [J·kg^{-1}·K^{-1}] and t - time [s] [26].

Assuming that the energy-transfer mechanism is purely conductive, the length of the trajectory of all particles is constant and equal to L, the plasma gas velocity is constant and the relative movement of particles correspond to *Stokes regime*, the integration of the eq. (3) leads to the following expression:

$$AHF = \frac{L\left(T_g - T_p\right)^2 \left(\langle \lambda_g \rangle\right)^2}{\langle \eta_g \rangle \, v_p} = \frac{{H_m}^2 {d_p}^2 \rho_p}{16} = DMF \quad (4)$$

in which L is length of high temperature zone of plasma jet [m], $\langle \lambda_g \rangle$ - average thermal conductivity [W.kg^{-1}·K^{-1}], $\langle \eta_g \rangle$ - dynamic viscosity [kg.m^{-1}·s^{-1}], v_p – particle velocity [m.s^{-1}], ${H_m}^2$ – total enthalpy of fusion [J.kg-1], d_p – particle diameter [m], ρ_p – particle density [kg.m^{-3}] [26]. The variables of the integration are separated into two parameters: on the left hand, the variables related to the plasma plume are collected in a parameter called ability of heating factor (*AHF*) while on the right hand the solid properties are collected and they defined another parameter named Difficulty of Melting Factor (*DFM*). The whole fusion of the solid occurs when *AHF* is equal or greater to *DFM*.

One approach assumed in the integration of eq. (3) is that the transport properties of the gas at the interface solid particle-plasma plume are averaged between the temperature of the gas (T_g) and the temperature of the particle surface (T_p). Therefore, the averaged

thermal conductivity and average viscosity, can be calculated from the following expression:

$$\langle \lambda_g \rangle = \frac{1}{T_g - T_p} \int_{T_p}^{T_g} \lambda_g(T) \mathrm{d}T \quad (5)$$

$$\langle \eta_g \rangle = \frac{1}{T_g - T_p} \int_{T_p}^{T_g} \eta_g(T) \mathrm{d}T$$

The *AHF* results an interesting factor to estimate the possibility of obtaining dense coatings [19,26]. Thus, it has been considered in the present study but the final calculations were modified to only take the transport coefficients and is expressed as:

$$AHF_{mod} = \frac{1}{(T_g - T_p)} \sqrt{\frac{AHF \cdot v_g}{L}} = \frac{\langle \lambda_g \rangle}{\langle \eta_g \rangle^2} \quad (6)$$

3. Results and discussion

3.1. Study of plasma plume composition

Prior to studing the transport properties, the composition of the plasma plume at different temperatures is analyzed in order to explain later the motives of the properties changes. In the calculation, it was assumed a flow rate of plasma working gases Ar + H_2 equal to 45 + 5 slpm, a solution feed rate of 50 mL/min and a solution concentration of 2 mol/L, values token from previous experimental works [22,27].

Fig. 1 shows the plasma plume composition at different temperatures using an inorganic precursor (zirconyl chloride) and an organic precursor (zirconium acetate). The precursor decomposition to zirconia and the secondary compound, hydrogen chloride (HCl) or methane (CH_4), occurs at low temperatures. Nevertheless, the molar ration of these compounds is poorly significant compared to the initial working gases or the steam. It is important to note that water concentration depends on molarity but also on the precursor compound since solutions of big molecules with high mole number (as

zirconium acetate with *M*=327.2 g/mol) need less amount of water to obtain the same solution molarity.

The water decomposition in atomic hydrogen and oxygen begins at about 3000K, as it is shown in eq. 7:

$$H_2O \rightarrow H^+ + OH^- \rightarrow 2H + O \quad (7)$$

These atomic species, concretely atomic hydrogen, really are excited (its kinetic energy is really high) therefore, increase the mobility, i.e. the thermal conductivity, inside the plasma plume [28]. High hydrogen ratio on the plasma working gases or high amount of water into the solution feedstock increase the plasma thermal conductivity.

In the case of organic precursors, oxidation occurs at high temperatures (around 6000 K), as it is described in eq. 8 [29]:

$$CH_4 + {}^1/_2\, O_2 \rightarrow CO + 2\, H_2 \rightarrow C + O + 4H \quad (8)$$

Thus, the decomposition of organic compounds creates also diatomic molecules and, after highly excited atoms, but the latter phenomenon occurs at higher temperatures, and and it is less significant since amount of methane in the gas mixture is considerable lower than the amount of water and hydrogen.

3.2. Effect of the composition on transport properties

The transport properties, such as viscosity and thermal conductivity, of the plasma plume are compared considering the different solution precursors displayed in Table 1. The considered working mixture, feedstock flow rate and molarities are equal to those in section 3.1. The results of dynamic viscosity calculus are collected in Fig. 2. This property is hardly modified by the composition variation, being the mixture with a higher molecular weight (zirconium acetate) the composition which displays a lower viscosity. Besides, a small negative peak of viscosity was observed at 3600 K which is

attributed to the presence of the OH^- radicals due to the decomposition of water steam [19,29]. This peak is less marked in mixtures with lower amount of water (zirconium acetate) or it is imperceptible in the case of pure working gases.

On the other hand, the composition exhibited a strong effect on thermal conductivity, as it is shown in Fig. 3. A noteworthy peak appears near 3000K owing to the generation of atomic hydrogen. Thus, feedstocks mixtures with higher amount of water (higher dilutions or smaller molecules as chloride) considerably increase the thermal conductivity [28]. Another secondary peak around 6000 K is appreciated just using an organic precursor as feedstock. This singularity is due to the final decomposition of organic compounds in C, H and O atoms. However, this secondary peak is less marked than the first mentioned. The appreciation of this secondary peak agrees with previous studies which concluded that a similar peak is observed using ethanol as solvent instead of water [29]. It is important to highlight the thermal conductivity is an important property to take into account in the SPPS technique, rather than in the conventional APS technique, since the spraying distances are relatively shorts (40-60 mm instead of 80-120 mm used for coarse powder spraying) [7,9].

Besides the transport properties, the modified ability of heating factor is also calculated, as it can be observed in Fig. 4, with the aim of evaluating the heat flux between the plasma and the feedstock. The AHF_{mod} is 3 times, or more, greater for the working gases including the precursors than for pure $Ar+H_2$ plasma. This factor increases near 3000 K because of the hydrogen dissociation and it reaches its maximum near 4000 K. Then, AHF_{mod} is slightly reduced at higher temperatures and the decomposition of organic compounds into elements is hardly reflected in this factor. In conclusion, the compositions which provide a higher amount of hydrogen atoms exhibit a greater *AHF*.

3.3. Effect of the concentration and flow rate on transport properties

The zirconium acetate is taken as feedstock for this part of the study. The effect of the concentration and flow rate on transport properties was studied considering other precursors and the results were similar. The considered solution concentrations and the feedstock flow rates are shown in Table 1. These parameters hardly affect viscosity but their effect is visible in thermal conductivity and in the ability of heating factor displayed in Fig. 5 and Fig. 6 respectively. The main peak in thermal conductivity is more marked at higher flow rates or lower concentrations, it means when the amount of water inside the precursor is higher. However, the secondary peak is greater at higher flow rates, as occurs in the main peak, but the concentration plays an opposite effect, being favorable a higher concentration. The reason is that the secondary peak is caused by the decomposition of the organic part and it increases at higher flow rate or concentrations. Regarding the *AHF*, a pronounced increment between 3000 and 4000 K is observed. Besides, the secondary peak is hardly appreciated (the gradient is just 1 % in the case of 4 mol/L solutions). AHF is 35 % greater increasing twice the flow rate and reducing the concentration. It means a higher heat flux between the plasma and the feedstock, an important consideration in SPPS technique, and it modifies the phenomena which occurs inside the plasma plume. Nevertheless, energetic

considerations should be taken into account since compositions with a higher amount of solvent need a more energetic plasma to evaporate it [8].

The effect of the concentration and flow rate on transport properties was studied considering other precursors and the results were similar.

4. Conclusions

Transport properties allow to estimate the heat and momentum transfer between the plasma plume and the feedstock. These properties depends on the chemical composition of the plasma plume and they are strongly modified when a liquid feedstock is injected.

- A marked increment of the thermal conductivity, therefore of the ability of heating factor, is produced in the SPPS technique when a solution is injected inside the plasma plume. The reason is based on the decomposition of molecular H_2O into highly energetic radicals at 3000 K. Thus the increase is more notable when the feedstock has a greater amount of water. It does not just imply a higher

feedstock flow rate or a lower solution concentration, but precursors with a smaller molecule size.

- The decomposition of organic compounds also contributed to the increment of thermal conductivity but it hardly affects the ability of heating factor.
- Plasma plume viscosity is less sensible to precursor variation than thermal conductivity.

Definitively, the estimation to transport properties, linked to the energetic requirements, can explain the phenomena which occur inside the plasma plume in a plasma deposition technique.

Acknowledgment

P. Carpio acknowledges the Valencia Government (APOSTD/2016/040) and the Spanish Ministry of Science, Innovation and Universities for his current post-doc contract (FJCI-2016-27822) for his post-doc contract.

References

[1] M. Gell, E.H. Jordan, M. Teicholz, B.M. Cetegen, N.P. Padture, L. Xie, D. Chen, X. Ma, J. Roth, Thermal barrier coatings made by the solution precursor plasma spray process, J. Therm. Spray Technol. 17 (2008) 124–135. doi:10.1007/s11666-007-9141-5.

[2] A. Joulia, G. Bolelli, E. Gualtieri, L. Lusvarghi, S. Valeri, M. Vardelle, S. Rossignol, A. Vardelle, Comparing the deposition mechanisms in suspension plasma spray (SPS) and solution precursor plasma spray (SPPS) deposition of yttria-stabilised zirconia (YSZ), J. Eur. Ceram. Soc. 34 (2014) 3925–3940. doi:10.1016/j.jeurceramsoc.2014.05.024.

[3] C. Zhang, X. Geng, H. Li, P.J. He, M.P. Planche, H. Liao, M.G. Olivier, M. Debliquy, Microstructure and gas sensing properties of solution precursor plasma-sprayed zinc oxide coatings, Mater. Res. Bull. 63 (2015) 67–71. doi:10.1016/j.materresbull.2014.11.044.

[4] K. Chien, T.W. Coyle, Rapid and continuous deposition of porous nanocrystalline SnO2coating with interpenetrating pores for gas sensor applications, J. Therm. Spray Technol. 16 (2007) 886–892. doi:10.1007/s11666-007-9076-x.

[5] R.T. Candidato, L. Pawlowski, P. Sokolowski, G. Lecomte-nana, C. Constantinescu, A. Denoirjean, Development of high purity hydroxyapatite coatings by solution precursor plasma spray process, (2015) 1–11. doi:10.1016/j.surfcoat.2016.10.072.

[6] Y. Xiao, L. Song, X. Liu, Y. Huang, T. Huang, J. Chen, Y. Wu, F. Wu, Bioactive glass-ceramic coatings synthesized by the liquid precursor plasma spraying process, J. Therm. Spray Technol. 20 (2011) 560–568. doi:10.1007/s11666-010-9594-9.

[7] L. Pawłowski, Application of solution precursor spray techniques to obtain ceramic films and coatings, Elsevier Ltd., 2015. doi:10.1016/B978-0-85709-769-9.00005-1.

[8] E.H. Jordan, C. Jiang, M. Gell, The Solution Precursor Plasma Spray (SPPS) Process: A Review with Energy Considerations, J. Therm. Spray Technol. 24 (2015) 1153–1165. doi:10.1007/s11666-015-0272-9.

[9] A. Killinger, R. Gadow, G. Mauer, A. Guignard, R. Vaen, D. Stöver, Review of new developments in suspension and solution precursor thermal spray processes, J. Therm. Spray Technol. 20 (2011) 677–695. doi:10.1007/s11666-011-9639-8.

[10] D. Chen, E.H. Jordan, M. Gell, The solution precursor plasma spray coatings: Influence of solvent type, Plasma Chem. Plasma Process. 30 (2010) 111–119. doi:10.1007/s11090-009-9200-4.

[11] C.K. Muoto, E.H. Jordan, M. Gell, M. Aindow, Identification of desirable precursor properties for solution precursor plasma spray, J. Therm. Spray

Technol. 20 (2011) 802–816. doi:10.1007/s11666-011-9636-y.

[12] C.S. Ramachandran, V. Balasubramanian, P. V. Ananthapadmanabhan, Multiobjective optimization of atmospheric plasma spray process parameters to deposit yttria-stabilized zirconia coatings using response surface methodology, J. Therm. Spray Technol. 20 (2011) 590–607. doi:10.1007/s11666-010-9604-y.

[13] C. Marchand, C. Chazelas, G. Mariaux, A. Vardelle, Liquid precursor plasma spraying: Modeling the interactions between the transient plasma jet and the droplets, J. Therm. Spray Technol. 16 (2007) 705–712. doi:10.1007/s11666-007-9112-x.

[14] X. Chen, Heat and Momentum Transfer between Thermal Plasma and Suspended Particles for different Knudsen Numbers, Thin Solid Films. 345 (1999) 140–145.

[15] H.B. Xiong, L.L. Zheng, S. Sampath, R.L. Williamson, J.R. Fincke, Three-dimensional simulation of plasma spray: Effects of carrier gas flow and particle injection on plasma jet and entrained particle behavior, Int. J. Heat Mass Transf. 47 (2004) 5189–5200. doi:10.1016/j.ijheatmasstransfer.2004.07.005.

[16] Y. Hu, Y. Shan, Modeling of Solution Droplet Evolution and Particle Morphologies in Solution Plasma Spraying, (n.d.).

[17] A. Saha, S. Seal, B. Cetegen, E. Jordan, A. Ozturk, S. Basu, Surface & Coatings Technology Thermo-physical processes in cerium nitrate precursor droplets injected into high temperature plasma, Surf. Coat. Technol. 203 (2009) 2081–2091. doi:10.1016/j.surfcoat.2008.09.018.

[18] B. Pateyron, L. Pawłowski, N. Calve, G. Delluc, A. Denoirjean, Modeling of phenomena occurring in plasma jet during suspension spraying of hydroxyapatite coatings, Surf. Coatings Technol. 214 (2013) 86–90. doi:10.1016/j.surfcoat.2012.11.006.

[19] B. Pateyron, N. Calve, L. Paw, Surface & Coatings Technology In fl uence of water and ethanol on transport properties of the jets used in suspension plasma spraying, 220 (2013) 257–260. doi:10.1016/j.surfcoat.2012.10.010.

[20] Y. Wang, T.W. Coyle, Solution precursor plasma spray of nickel-yittia stabilized zirconia anodes for solid oxide fuel cell application, J. Therm. Spray Technol. 16 (2007) 898–904. doi:10.1007/s11666-007-9108-6.

[21] Y. Wang, T.W. Coyle, Optimization of solution precursor plasma spray process by statistical design of experiment, J. Therm. Spray Technol. 17 (2008) 692–699. doi:10.1007/s11666-008-9227-8.

[22] S. V. Joshi, G. Sivakumar, T. Raghuveer, R.O. Dusane, Hybrid plasma-sprayed thermal barrier coatings using powder and solution precursor feedstock, J. Therm. Spray Technol. 23 (2014) 616–624. doi:10.1007/s11666-014-0075-4.

[23] E.A. Mason, R.J. Munn, Transport coefficients of ionized gases, Phys. Fluids. 10

(1967) 1827.

[24] http://ttwinner.free.fr/en/home.html, (n.d.).

[25] W.B. White, S.M. Johnson, G.B. Dantzig, Chemical equilibrium in complex mixtures, J. Chem. Phys. 28 (1958) 751.

[26] L. Pawlowski, The Science and Engineering of Thermal Spray Coating, 2nd ed., Wiley, Chichester, 2008.

[27] S. Kozerski, L. Łatka, L. Pawlowski, F. Cernuschi, F. Petit, C. Pierlot, H. Podlesak, J. Paul, Preliminary study on suspension plasma sprayed ZrO 2 + 8 wt .% Y 2 O 3 coatings, J. Eur. Ceram. Soc. 31 (2011) 2089–2098. doi:10.1016/j.jeurceramsoc.2011.05.014.

[28] V. Rat, A.B. Murphy, J. Aubreton, M.F. Elchinger, P. Fauchais, Treatment of non-equilibrium phenomena in thermal plasma flows, J. Phys. D. Appl. Phys. 41 (2008). doi:10.1088/0022-3727/41/18/183001.

[29] B. Pateyron, G. Delluc, P. Fauchais, Chemical and transport properties of carbon-oxygen-hydrogen plasmas in isochoric conditions, Plasma Chem. Plasma Process. 25 (2005) 485–502. doi:10.1007/s11090-005-4994-1.

Table

Table 1. Type of precursor, the molarity and flow rate values contemplated in the thermal transport estimations.

Kind of precursor	**Molarity**	**Solution flow rate**
(2 mol/L and 50 mL/min)	(zirconium acetate)	
• Zirconium acetate [$Zr(CH_3COO)_4$] • Zirconyl nitrate [$ZrO(NO_3)_2$] • Zirconyl chloride [$ZrOCl_2$]	• 2 mol/L • 4 mol/L	• 30 mL/min • 50 mL/min

Figure captions

Figure 1. Plasma plume composition injecting different solutions: bottom) zirconium acetate; top) zirconyl chloride. Minor species are represented in a reduced Y-axis scale graph.

Figure 2. Dynamic viscosity of the plasma plume injecting different precursors.

Figure 3. Thermal conductivity of the plasma plume injecting different precursors.

Figure 4. Modified ability of heating factor of the plasma plume injecting different precursors.

Figure 5. Thermal conductivity of the plasma plume at different feedstock flow rates and concentrations.

Figure 6. Modified ability of heating factor of the plasma plume at different feedstock flow rates and concentrations.

Figure

Figure 1

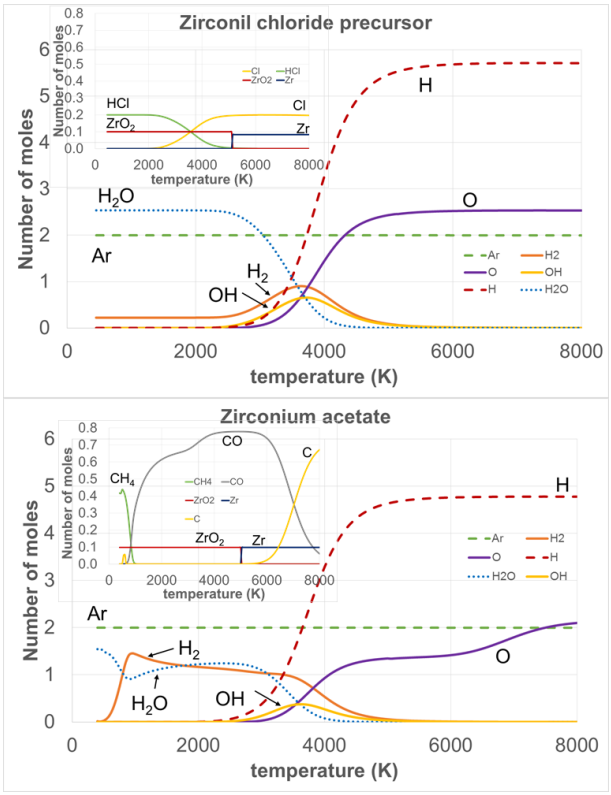

Figure 2

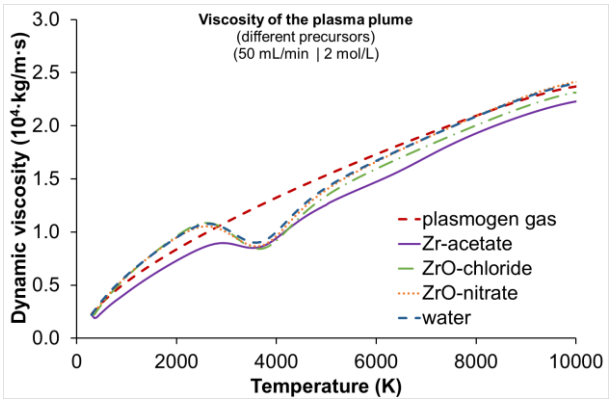

Figure 3

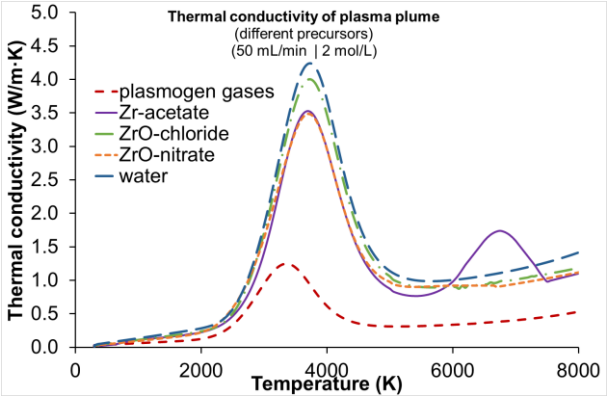

Figure 4

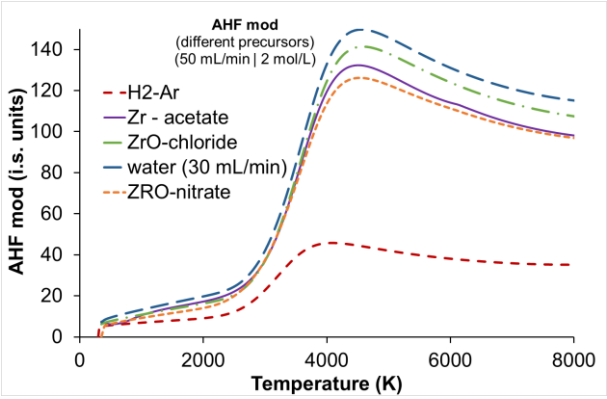

Figure 5

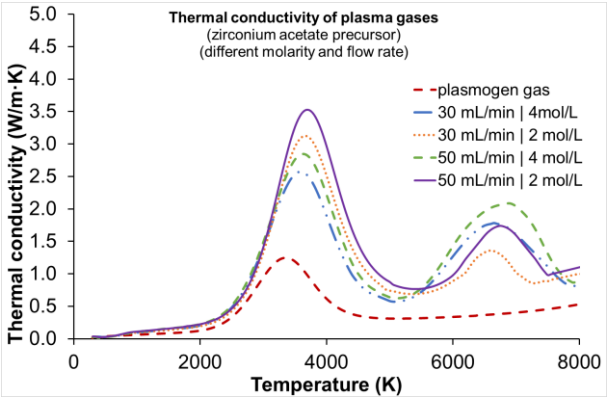

Figure 6

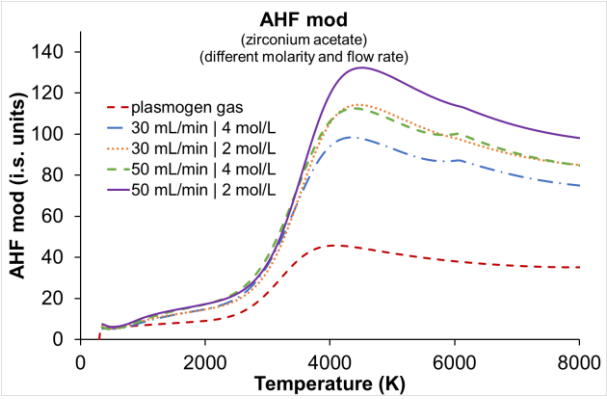
AHF mod
(zirconium acetate)
(different molarity and flow rate)
plasmogen gas
30 mL/min | 4 mol/L
30 mL/min | 2 mol/L
50 mL/min | 4 mol/L
50 mL/min | 2 mol/L
AHF mod (i.s. units)
Temperature (K)
0
20
40
60
80
100
120
140
0
2000
4000
6000
8000